Hindawi Publishing Corporation
EURASIP Journal on Wireless Communications and Networking
Volume 2006, Article ID 40264, Pages 1–7
DOI 10.1155/WCN/2006/40264

Robust OFDM System with ml-HIM Encoding

M. J. Dehghani

Department of Electrical Engineering, Shiraz University of Technology, Modarres Boulevard, P.O. Box 313, Shiraz 71555, Iran

Received 10 April 2006; Revised 16 July 2006; Accepted 22 September 2006

Recommended for Publication by Mischa Dohler

Differential encoding is a widely used technique in the context of orthogonal frequency division multiplexing (OFDM) as an alternative to coherent channel estimation and equalization. In this paper, the performance of differential encoding using a multilag higher-order instantaneous moment (ml-HIM) in OFDM system is investigated. It is shown that by using proper order and lags, the ml-HIM decoder is capable to make a robust system against the phase distortion and the intercarrier interference (ICI) caused by phase distortion and frequency offset.

1. INTRODUCTION

OFDM systems have generated a lot of interest in diverse digital communication applications. This has been due to favorable properties such as high spectral efficiency by allowing overlap, robustness against intersymbol interference (ISI) and resistance to impulse noise, ability to dynamically optimize the rate to the channel specifications and high computational efficiency by using the fast Fourier transform (FFT) technique to implement the modulation and demodulation functions [1]. The OFDM has also been exploited for wideband data communication over mobile radio frequency modulation (FM) channels, asymmetric digital subscriber lines (ADSL), very high data digital subscriber lines (VDSL) [2], and digital audio broadcasting (DAB) [3].

While inherently robust against multipath fading, OFDM has some disadvantages with respect to single carrier systems. In particular, it has a larger peak-to-average signal power ratio than single carrier modulation and a correspondingly larger sensitivity to nonlinear distortions in a high power amplifier [4]. In addition, it exhibits serious degradations when the carrier frequency offset is not accurately estimated and compensated [5, 6]. Phase ambiguity and/or frequency errors are likely to be present in the received signal due to imperfect knowledge of the frequency and phase of the carrier, fading effects, or multipath propagation. Typically, phase distortions are captured in the term $e^{j\theta_c(t)}$, which multiplies the received baseband signal. When phase variations are induced by the relative motion between the transmitter and the receiver (such as in mobile and satellite communications), the phase $\theta_c(t)$ is a polynomial in terms of continuous time t, and its coefficients are related to the kinematics of the moving station [7].

As an alternative to modeling and estimating phase distortions, phase errors can be precompensated by differential encoding and decoding. Currently, differential encoding is used in the context of OFDM as an alternative to coherent channel estimation and equalization. The European digital audio broadcast (DAB) standard employs differential encoding [3]. Although tolerant to constant phase errors, differential detection systems are sensitive to carrier frequency variations. To overcome this problem, doubly differential phase shift keying (DDPSK) in single carrier modulation has been introduced [8]. Since in applications such as low earth orbiting (LEO) satellite communications [9], the Doppler frequency also changes with time, these approaches are not sufficient for compensation. Algorithms for frequency and frequency rate-of-change estimation are proposed [10], based on Lanczos FIR differentiators, but they suffer from nonnegligible estimation bias. Generalizations to higher-than-second-order M-ary DPSK have also been suggested in [11]. An interesting approach to carrier frequency and synchronization acquisition has been proposed for OFDM systems [12], which is tolerant to time-variant Doppler frequency.

The multilag higher-order instantaneous moment (ml-HIM) is a transformation originally studied in [13]. It is a generalized differential encoding technique which has been applied to M-ary PSK and QAM in single carrier modulation

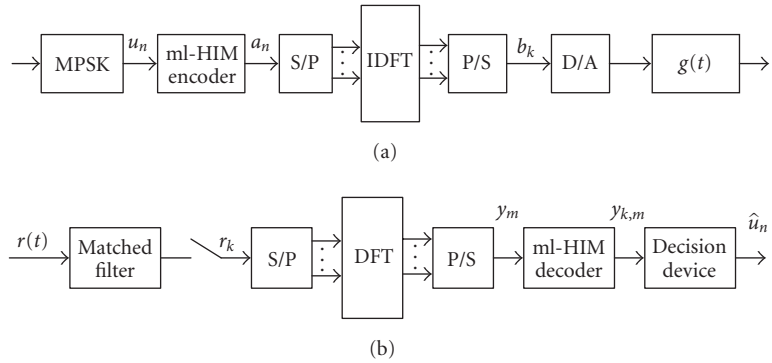

Figure 1: Functional block diagram of the considered OFDM on differential encoding (ml-HIM) over adjacent subcarriers: (a) transmitter, (b) receiver.

[14]. In this paper, we propose to incorporate ml-HIM encoding and decoding in an OFDM system to combat not only carrier frequency offset and phase offset, but also other phase distortions. We have applied multilag HIM in the frequency domain as differential encoding and decoding over adjacent subcarriers to PSK signaling in the OFDM transceiver. In order to simulate a distortion phase in transmission signal, we have provided a nondispersive channel. We have shown that, in comparison to conventional differential encoding (DPSK), the degrees of freedom offered by the different lags in the ml-HIM technique are able to make robust against the intercarrier interference (ICI) caused by phase distortion. To improve the performance of the system, we can concatenate the proposed system with error-correcting coding or turbo codes (TCs), which for simplicity have been excluded from the proposed system.

This paper is organized as follows: in Section 2, we review the main features of OFDM and consider the relationship between the information and the transmitted symbols with phase ambiguity or phase distortion due to imperfect knowledge of the carrier's phase and frequency. Section 3 reviews multilag HIM encoding and decoding in a general case for M-ary PSK. Section 4 applies ml-HIM as a differential encoding to an OFDM system in the frequency domain and derives some expressions for the received signal in different situations. In the same section, we have investigated the system performance in terms of ml-HIM lags or delays and have determined proper lags through computer simulation. In Section 5, results and conclusions are presented.

2. SYSTEM OUTLINE

Figure 1 shows the baseband functional block diagram of the OFDM transceiver which is considered in this paper. The differential or ml-HIM encoding can be applied over adjacent OFDM symbols, or over adjacent subcarriers (as shown in Figure 1(a)), or both methods can be combined [15]. The incoming serial binary data is first grouped into b-bits and each group is converted into a complex number by using the signal constellation, say, for example, multiphase shift keying (MPSK, $b = \log_2 M$). The complex symbols are differentially encoded, converted from serial to parallel, given guard interval insertion to avoid intersymbol interference (ISI) by multipath distortion, and modulated in a baseband fashion by the IDFT. Each block of frequency-domain symbols is used to produce a corresponding block of channel symbols b_k, $k = 0, 1, \ldots, N-1$, through an IDFT, as follows:

$$b_k = \frac{1}{\sqrt{N}} \sum_{n=0}^{N-1} a_n e^{j2\pi kn/N}, \quad k = 0, 1, \ldots, N-1. \tag{1}$$

The symbols are converted back to serial data and then passed through the transmission filter, whose impulse response $g(t)$ depends on the characteristics of the channel, particularly on channel spacing. By a proper choice of time origin, the complex envelope of the signal transmitted in the generic block can be written as [12]

$$x(t) = \sum_{k=0}^{N-1} b_k g(t - kT_s), \tag{2}$$

where T_s is the symbol period. The receiver performs the reverse function of the transmitter (Figure 1(b)). In the presence of a distorting phase between the carrier frequency and the local oscillator, the received signal under the assumption of ideal frame recovery after baseband conversion (not shown) is [12, 14]

$$r(t) = x(t)e^{j\theta_c(t)} + w(t), \tag{3}$$

where $\theta_c(t)$ models the composite phase error introduced by the channel and the imperfect knowledge of the frequency and phase of the carrier; and $w(t)$ is the additive white Gaussian noise (AWGN) with two-sided normalized power spectral density $N_0/2P_s$ where P_s and N_0 denote the average signal power and noise power, respectively. Suppose a second-order approximation represents an accurate model of $\theta_c(t)$, such that [14]

$$\theta_c(t) = \theta_0 + 2\pi f_d t + \pi \alpha_d t^2, \tag{4}$$

with θ_0 denoting the phase offset; f_d and α_d are the Doppler shift and Doppler rate, respectively. Higher order phase polynomials can be considered as well. With $\theta_c(t)$ given by (4),

model (3) holds, provided that Doppler frequency and the Doppler rate are small when compared to the symbol rate, which is a condition satisfied in many practical cases [14]. After matched filtering, we assume that the signal is sampled, and the sampler output is written as

$$r_k = b_k e^{j\theta_k} + n_k, \quad k = 0, 1, \ldots, N-1, \tag{5}$$

where θ_k is given by

$$\theta_k = \theta_0 + 2\pi f_e k + \pi \alpha_e k^2, \quad k = 0, 1, \ldots, N-1. \tag{6}$$

Here, $\theta_k = \theta(kT_s)$, $r_k = r(kT_s)$, $f_e = f_d T_s$, $\alpha_e = \alpha_d T_s^2$, and n_k represents zero-mean complex Gaussian noise with independent real and imaginary components, each of variance $N_0/2P_sT_s$. The signal r_k is then fed to the DFT block, yielding

$$y_m = \frac{1}{\sqrt{N}} \sum_{k=0}^{N-1} r_k e^{-j2\pi mk/N}, \quad m = 0, 1, \ldots, N-1. \tag{7}$$

Substituting (1) and (5) in (7), we have the following relation:

$$\begin{aligned} y_m &= \frac{1}{\sqrt{N}} \sum_{k=0}^{N-1} \left(b_k e^{j\theta_k} + n_k\right) e^{-j2\pi mk/N} \\ &= \frac{a_m}{N} \sum_{k=0}^{N-1} e^{j\theta_k} + \frac{1}{N} \sum_{k=0}^{N-1} \sum_{n=0, n\neq m}^{N-1} a_n e^{j\theta_k} e^{j2\pi(n-m)k/N} + \eta_m, \\ &\qquad m = 0, 1, \ldots, N-1, \end{aligned} \tag{8}$$

where $\eta_m = (1/\sqrt{N}) \sum_{k=0}^{N-1} n_k e^{-j2\pi k/N}$; it represents Gaussian noise with the same statistics as n_k. The signal y_m can be expressed as a sum of the desired signal C_m, the two undesired signals, the ICI signal I_m, and noise signal η_m, that is, $y_m = C_m + I_m + \eta_m$, where

$$\begin{aligned} C_m &= a_m \frac{1}{N} \sum_{k=0}^{N-1} e^{j\theta_k}, \\ I_m &= \frac{1}{N} \sum_{k=0}^{N-1} \sum_{n=0, n\neq m}^{N-1} a_n e^{j\theta_k} e^{j2\pi(n-m)k/N}. \end{aligned} \tag{9}$$

The desired signal value C_m depends only on the signal transmitted on subcarrier m, while I_m depends on the signals transmitted on the other subcarriers. The sequence $\{y_m\}$ is in turn applied to a differential detector or ml-HIM decoder whose output drives the decision device.

3. DIFFERENTIAL ENCODING WITH MULTILAG HIM

The multilag HIM technique can be applied to constant modulus constellations, such as MPSK, as well as to generic (nonconstant modulus) constellations, such as M-ary QAM. For the application of the ml-HIM technique to M-PSK signaling, let us assume the information symbols $u_m = e^{j\varphi_m}$ to be independent and identically distributed (i.i.d.), drawn from a discrete M-ary equiprobable PSK alphabet. The ml-HIM encoder converts the information sequence $\{u_m\}$ into

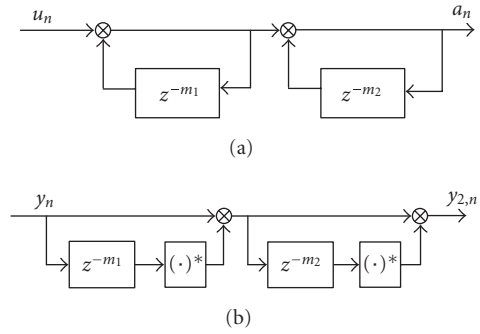

Figure 2: Second-order ml-HIM: (a) encoder, (b) decoder.

$\{a_m\}$, while the received noisy signal $\{y_m\}$ is decoded by the appropriate ml-HIM decoder. The first-order ml-HIM encoding and decoding, respectively, are specified as [14]

$$a_m = u_m a_{m-m_1}, \tag{10a}$$

$$w_{1,m} = y_m y^*_{m-m_1}, \tag{10b}$$

the second order as

$$a_m = u_m a_{m-m_1} a_{m-m_2} a^*_{m-m_1-m_2}, \tag{11a}$$

$$w_{2,m} = w_{1,m} w^*_{1,m-m_2} = y_m y^*_{m-m_1} y^*_{m-m_2} y_{m-m_1-m_2}, \tag{11b}$$

and the third order as

$$\begin{aligned} a_m &= u_m a_{m-m_1} a_{m-m_2} a_{m-m_3} a^*_{m-m_1-m_2} \\ &\quad \times a^*_{m-m_1-m_3} a^*_{m-m_2-m_3} a_{m-m_1-m_2-m_3}, \\ w_{3,m} &= w_{2,m} w^*_{2,m-m_3}, \end{aligned} \tag{12}$$

where $w_{l,m}$ is the output of the lth-order ml-HIM decoder, $(\cdot)^*$ denotes complex conjugation, and m_1, m_2, m_3 are lags or delays. To ensure causality, we select $1 \le m_1 \le m_2 \le m_3$. We illustrate the second-order ml-HIM encoder and decoder in Figure 2.

To remove an Lth-order polynomial phase distortion, we must use an $(L+1)$th-order ml-HIM system [14, 16]. Therefore, to remove a constant phase ambiguity, it is sufficient to use a first-order ml-HIM system for encoding and decoding. The second-order ml-HIM system can suppress the effect of both the constant phase and Doppler frequency, while the third-order ml-HIM performs likewise with second-order phase distortion.

In all cases, the receiver chooses that symbol $\hat{u}_m$, which is closest to the noisy estimate $w_{l,m}$ of u_m, that is, the decision rule (ML) is given by

$$\hat{u}_m = \underset{u_m}{\operatorname{argmin}} \left| u_m - w_{l,m} \right|, \tag{13}$$

where argmin $(\cdot)$ yields the argument for which the given expression achieves the global minimum.

4. SIMULATION DETAILS AND RESULTS

In the following pages, we simulate data transmission in a wireless, mobile environment with different phase distortions. The bit rate is 128 kb/s with 128 *subcarriers*. We have

assumed a binary PSK constellation in all the cases with average signal power of $E\{|u_m|^2\}$ and complex AWGN noise with independent zero-mean real and imaginary components, each of variance $\sigma^2/2$. The BER performance is measured for several values of the signal-to-noise ratios (SNRs), which are defined as $E\{|u_m|^2\}/\sigma^2$ with u_m having unit magnitude. To obtain the results for a target BER of 10^{-4}, we have used Monte-Carlo simulation technique with 10^5 symbols for each set of lags.

4.1. First-order ml-HIM for removing carrier phase offset

Consider the case of M-ary PSK signaling as in Section 2. Assume that the phase distortion in (6) has order zero, that is, $f_e = 0$, $\alpha_e = 0$, and then $\theta_k = \theta_0$, with the assumption of ideal carrier recovery. In this case, the encoding and decoding strategy is given by (10a) and (10b), respectively. Substituting $\theta_k = \theta_0$ in (8), the received signal has the simple form

$$y_m = a_m e^{j\theta_0} + \eta_m, \quad m = 0, 1, \ldots, N-1. \tag{14}$$

Equation (14) shows there is no ICI in the output signal in any subcarrier. The decision is based on the noisy estimate of u_m, that is,

$$w_{1,m} = y_m y^*_{m-m_1} = u_m + \zeta(m_1), \tag{15}$$

where $\zeta(m_1)$ denotes the disturbance term, which is

$$\zeta(m_1) = e^{j\theta_0} a_m \eta^*_{m-m_1} + e^{-j\theta_0} a^*_{m-m_1} \eta_m + \eta_m \eta^*_{m-m_1}. \tag{16}$$

When u_m is drawn from an MPSK constellation and η_m is a zero-mean complex AWGN with variance σ^2, then $\zeta(m_1)$ has zero mean. We define the deflection D as a performance criterion function in detection as suggested in [14], that is,

$$D = \frac{\text{var}\{u_m\}}{\text{var}\{\zeta(m_1)\}} = \frac{E\{|u_m|^2\}}{E\{|\zeta(m_1)|^2\}}. \tag{17}$$

The goal is to find the lag m_1 that maximizes the deflection function D. Substituting (15) and (16) in (17), we obtain $D = 1/(2\sigma^2 + \sigma^4)$ which is independent of θ_0 and m_1. Figure 3 shows the BER performance in terms of SNR for $\theta_0 = \pi/6$ and in terms of the lags $m_1 = 1, 2$. As expected, the system has the same BER performance for different lags. A good choice for the lag is $m_1 = 1$, because it minimizes the number of symbols required to initialize the differential decoder. In the case $m_1 = 1$, the transceiver is the same as standard binary DPSK applied over adjacent subcarriers in the OFDM system. According to Figure 3, for a BER of about 10^{-4}, about 0.8 dB of additional SNR is required when the first-order ml-HIM system is used, when compared to the ideal BPSK (with $\theta_0 = 0$ and $f_e = 0$).

4.2. Second-order ml-HIM for removing carrier phase and frequency offset

Let us consider the phase distortion of order one, that is, $\theta_k = \theta_0 + 2\pi f_e k$, which is first-order phase distortion. In this case, we need to apply second-order ml-HIM for encoding and decoding as given in (11a) and (11b), respectively. Substituting $\theta_k = \theta_0 + 2\pi f_e k$ in (8), we get

$$\begin{aligned} y_m &= \frac{1}{\sqrt{N}} \sum_{k=0}^{N-1} (b_k e^{j\theta_k} + n_k) e^{-j2\pi mk/N} \\ &= \frac{\sin(\pi f_e N)}{N \sin(\pi f_e)} e^{j(\theta_0 + \pi f_e (N-1))} a_m \\ &\quad + \frac{e^{j\theta_0}}{N} (1 - e^{j2\pi f_e N}) \sum_{n=0, n\neq m}^{N-1} \frac{a_m}{1 - e^{j2\pi(n-m+f_e N)/N}} + \eta_m, \\ &\qquad m = 0, 1, \ldots, N-1. \end{aligned} \tag{18}$$

Substituting (18) in (11a) and (11b) for the second-order system, we get

$$w_{2,m} = \left(\frac{\sin(\pi f_e N)}{N \sin(\pi f_e)} \right)^4 u_m + \zeta(m_1, m_2), \tag{19}$$

where $\zeta(m_1, m_2)$ is a disturbance term that is superimposed on the useful term u_m, which depends on the ICI, noise, and lags. The deflection function is defined as

$$D = \frac{E\{|C_m|^2\}}{E\{|\zeta(m_1, m_2)|^2\}}, \quad \text{where } C_m = \left(\frac{\sin(\pi f_e N)}{N \sin(\pi f_e)} \right)^4 u_m. \tag{20}$$

Comparison of the received sequence in (18) with (14) shows that the complexity in the ml-HIM of second order is much more than the first-order case. In order to calculate BER and the deflection function $D(m_1, m_2)$ and to obtain the optimal lags (m_1, m_2), we perform computer simulations. We assume that $\theta_0 = \pi/6$ and Doppler spread f_d to be 100 Hz. Therefore, we consider $\theta_k = \theta_0 + 2\pi f_e k$ with $f_e = f_d T_s = 7.8125 \times 10^{-4}$,

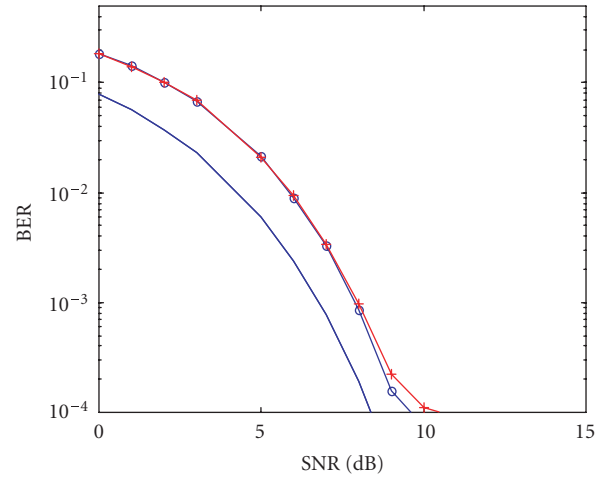

Figure 3: BER performance of second-order ml-HIM in BPSK-OFDM in terms of lags: circles ($m_1 = 1$), pluses ($m_1 = 2$). The solid line shows BER in ideal BPSK.

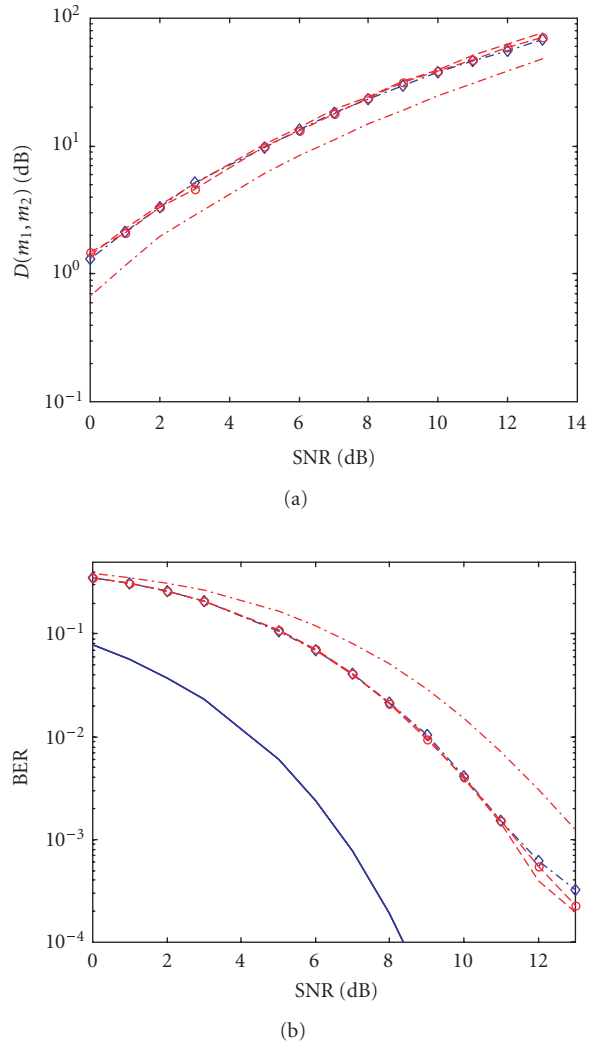

FIGURE 4: (a) Deflection function and (b) BER in second-order ml-HIM in terms of lags. Dash $(m_1, m_2) = (1, 1)$, circles $(1, 2)$, plus $(1, 3)$. The solid line shows BER for ideal BPSK.

which gives $C_m = 0.766u_m$. Figure 4 shows the deflection function and BER versus SNR for different lags $(m_1, m_2) = (1, 1), (1, 2)$, and $(1, 3)$. The results show that by selecting proper lags, good BER performance can be achieved. In comparison, it can be seen that except for $(m_1, m_2) = (1, 1)$, the values of the deflection functions and BERs for the other pairs of lags are equivalent. According to our results, the pair $(1, 1)$ which corresponds to DDPSK [8], is the worst in terms of BER performance. Considering the memory saved during initialization, $(m_1, m_2) = (1, 2)$ is a good choice for this ml-HIM encoder/decoder. In this case, for a BER of 10^{-4}, about 3.5 dB additional SNR is required when compared to the ideal BPSK, with $\theta_0 = 0$ and $f_e = 0$.

In order to investigate the effect of ICI on the system performance, we consider a noiseless environment, that is, $\eta_m = 0$, and focus on the contribution of ICI. The output sequence of the decoder is given by (19), where the disturbance term $\zeta(m_1, m_2)$ is the ICI. Thus the deflection function D becomes the carrier-to-interference power ratio (CIR) in this case. As expected, the simulation shows that the CIR of the ml-HIM system with lags $(m_1, m_2) = (1, 2)$ at 17.5 dB is 2.5 dB more than the CIR in the system with lags $(m_1, m_2) = (1, 1)$. Figure 4(a) shows the deflection functions for the different lags, where the CIR corresponds to the asymptotic values of these functions as SNR tends to infinity.

4.3. Third-order ml-HIM for removing second-order phase distortion

In this case, we use the phase distortion given in (6), that is, $\theta_k = \theta_0 + 2\pi f_e k + \pi\alpha_e k^2$. Therefore, we have considered phase and frequency offset, where the frequency offset due to Doppler frequency also changes with time. Substituting (6) in (8), the received signal is

$$y_m = \frac{a_m e^{j\theta_0}}{N} \sum_{k=0}^{N-1} e^{j(2\pi f_e k + \pi\alpha_e k^2)} + \frac{1}{N} \sum_{k=0}^{N-1} \sum_{n=0, n\neq m}^{N-1} a_n e^{j\theta_k} e^{j2\pi(n-m)k/N} + \eta_m. \tag{21}$$

To remove the effect of Doppler rate, Doppler frequency, and phase offset, the system needs to implement third-order ml-HIM encoding, as specified in (12). We get

$$\begin{aligned} w_{3,m} &= y_m y^*_{m-m_1} y^*_{m-m_2} y_{m-m_1-m_2} y^*_{m-m_3} \\ &\quad \times y_{m-m_1-m_3} y_{m-m_2-m_3} y^*_{m-m_1-m_2-m_3} \\ &= \left| \frac{1}{N} \sum_{k=0}^{N-1} e^{j(2\pi f_e k + \pi\alpha_e k^2)} \right|^8 u_m + \zeta(m_1, m_2, m_3), \end{aligned} \tag{22}$$

where $\zeta(m_1, m_2, m_3)$ is a disturbance term that is superimposed on the useful term u_m, which depends on the ICI, noise, and lags. The deflection function in this case is defined as

$$D = \frac{E\{|C_m|^2\}}{E\{|\zeta(m_1, m_2, m_3)|^2\}}, \quad \text{where } C_m = \left| \frac{1}{N} \sum_{k=0}^{N-1} e^{j(2\pi f_e k + \pi\alpha_e k^2)} \right|^8 u_m. \tag{23}$$

Because of the complexity of the disturbance term $\zeta(m_1, m_2, m_3)$, we resort to a computer-aided approach to evaluate the effect of the lags on the system performance. We assume that $\theta_0 = \pi/6$; the Doppler shift f_d and Doppler rate α_d are assumed to be 100 Hz and 200 $(\text{Hz})^{-2}$, respectively. Hence, $f_e = f_d T_s$ and $\alpha_e = \alpha_d T_s^2$ are calculated for $T_s = 1/128$ ms and $C_m = 0.585u_m$. Computer simulations show that the deflection function depends on the lags m_1, m_2, and m_3. The deflection D and BER are measured for different lags $(m_1, m_2, m_3) = (1, 1, 1), (1, 1, 2), (1, 2, 3)$ and $(2, 3, 4)$, as shown in Figure 5. The results show that maximum deflection and minimum BER are obtained only in the $(1, 2, 3)$ case. Hence, this is the best choice for the lags in third-order

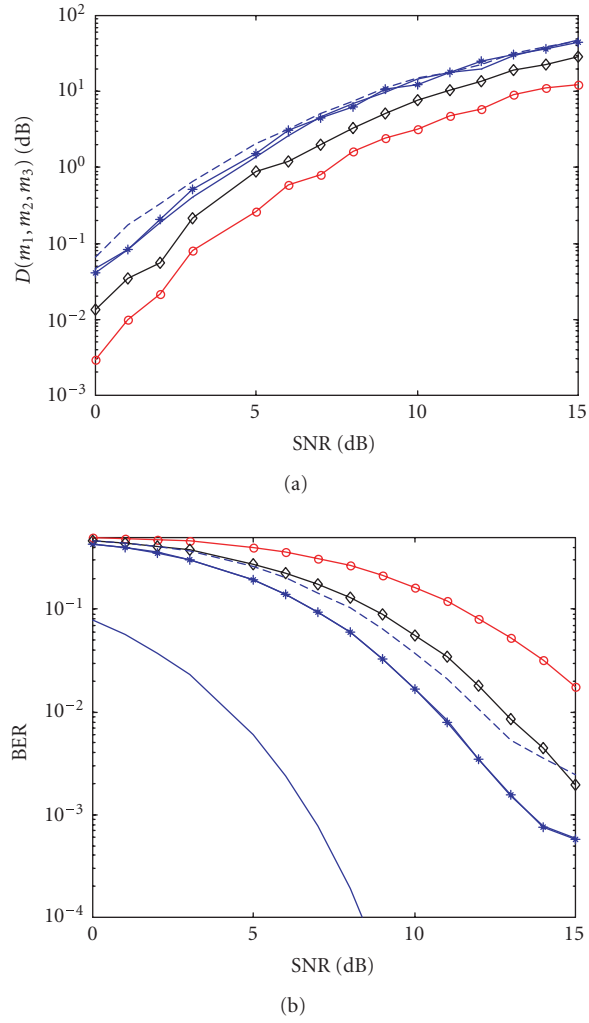

FIGURE 5: (a) Deflection function and (b) BER in third-order ml-HIM in terms of lags. Dash $(m_1, m_2, m_3) = (1, 1, 1)$, circles $(1, 2, 3)$, plus $(1, 1, 2)$, dot $(2, 3, 4)$. The solid line shows BER for ideal BPSK.

ml-HIM encoding. In this case, for a BER of 10^{-4}, about 7 dB additional SNR is required when compared to the ideal BPSK. In comparison, the $(1, 1, 2)$ and $(1, 1, 1)$ cases require 9 dB and 14 dB of additional SNR, respectively.

We have calculated the system in the noiseless case where $\eta_m = 0$, and have measured CIR for $(m_1, m_2, m_3) = (1, 1, 1)$ and $(1, 2, 3)$. As expected, the system has the best performance with lags of $(1, 2, 3)$. In comparison, the CIR for $(1, 1, 1)$ is about 9.5 dB, whereas for $(1, 2, 3)$ it is 14 dB. Hence, the ml-HIM system in the second case improves the CIR by 4.5 dB, and the CIR results are consistent with the BER, results. Figure 5(a) shows the deflection functions D for various lags, where once again the CIRs are the asymptotic values.

5. CONCLUSION

In this paper, the performance of differential encoding from a nonlinear signal processing perspective that relies on the multilag high-order instantaneous moment (ml-HIM) in OFDM systems is investigated. We have derived some expressions for the received signal in ml-HIM detection concatenated with OFDM system. In order to measure the BER and the ICI caused by phase distortion and also to determine the optimum lags, the maximum deflection criterion was used and we also considered different examples in our simulations. It has been shown that by using proper order and lags, the ml-HIM decoder is capable to make a robust OFDM system against the intercarrier interference (ICI) caused by phase distortions and frequency offset.

REFERENCES

[1] M. Faulkner, "The effect of filtering on the performance of OFDM systems," *IEEE Transactions on Vehicular Technology*, vol. 49, no. 5, pp. 1877–1884, 2000.

[2] J. A. C. Bingham, *ADSL, VDSL, and Multicarrier Modulation*, John Wiley & Sons, New York, NY, USA, 2000.

[3] P. Shelswell, "The COFDM modulation system: the heart of digital audio broadcasting," *Electronics and Communication Engineering Journal*, vol. 7, no. 3, pp. 127–136, 1995.

[4] M.-G. Di Benedetto and P. Mandarini, "An application of MMSE predistortion to OFDM systems," *IEEE Transactions on Communications*, vol. 44, no. 11, pp. 1417–1420, 1996.

[5] T. Pollet, M. Van Bladel, and M. Moeneclaey, "BER sensitivity of OFDM systems to carrier frequency offset and Wiener phase noise," *IEEE Transactions on Communications*, vol. 43, no. 234, pp. 191–193, 1995.

[6] M. Speth, S. A. Fechtel, G. Fock, and H. Meyr, "Optimum receiver design for wireless broad-band systems using OFDM-part I," *IEEE Transactions on Communications*, vol. 47, no. 11, pp. 1668–1677, 1999.

[7] A. W. Rihaczek, *Principles of High Resolution Radar*, Artech House, San Diego, Calif, USA, 1996.

[8] M. K. Simon and D. Divsalar, "On the implementation and performance of single and double differential detection schemes," *IEEE Transactions on Communications*, vol. 40, no. 2, pp. 278–291, 1992.

[9] A. Kajiwara, "Mobile satellite CDMA system robust to Doppler shift," *IEEE Transactions on Vehicular Technology*, vol. 44, no. 3, pp. 480–486, 1995.

[10] M. Mcintyre and A. Ashley, "A simple fixed-lag algorithm for tracking frequency rate of change," *IEEE Transactions on Aerospace and Electronic Systems*, vol. 29, no. 3, pp. 677–684, 1993.

[11] D. K. van Alphen and W. C. Lindsey, "Higher-order differential phase shift keyed modulation," *IEEE Transactions on Communications*, vol. 42, no. 234, part 1, pp. 440–448, 1994.

[12] M. Luise and R. Reggiannini, "Carrier frequency acquisition and tracking for OFDM systems," *IEEE Transactions on Communications*, vol. 44, no. 11, pp. 1590–1598, 1996.

[13] S. Barbarossa, A. Scaglione, and G. B. Giannakis, "Product high-order ambiguity function for multicomponent polynomial-phase signal modeling," *IEEE Transactions on Signal Processing*, vol. 46, no. 3, pp. 691–708, 1998.

[14] F. Gini and G. B. Giannakis, "Generalized differential encoding: a nonlinear signal processing perspective," *IEEE Transactions on Signal Processing*, vol. 46, no. 11, pp. 2967–2974, 1998.

[15] H. Schubert, A. Richter, and K. Iversen, "Differential modulation for OFDM in frequency Vs time domain," in *Proceedings of ACTS Mobile Communication Summit*, pp. 763–768, Aalborg, Denmark, October 1997.

[16] G. Zhou, G. B. Giannakis, and A. Swami, "On polynomial phase signals with time-varying amplitudes," *IEEE Transactions on Signal Processing*, vol. 44, no. 4, pp. 848–861, 1996.

M. J. Dehghani received the B.S. and M.S. degrees in electrical engineering from the Isfahan University of Technology, Iran, in 1988 and 1992, respectively. In 1993, he joined the faculty of Control Department, School of Electronic Technology, Shiraz University, Iran. He got his Ph.D. in the Electrical Engineering Department, IIT Madras, India in 2003. Since 2004, he has been on the faculty of the Department of Electrical Engineering, Shiraz University of Technology, Iran. His activities have included filter banks, high data-rate wireless communication, ADSL and OFDM systems as well as modem simulation studies. His interests are in the areas of communication systems and telecom applications of signal processing, space-time coding, and channel estimation.